THE JOURNAL OF PHYSICAL CHEMISTRY Letters

Letter

Cite This: J. Phys. Chem. Lett. 2018, 9, 7173−7179

pubs.acs.org/JPCL

Reversible Control of Chemoselectivity in $Au_{38}(SR)_{24}$ Nanocluster-Catalyzed Transfer Hydrogenation of Nitrobenzaldehyde Derivatives

Jianbo Zhao,[†,‡] Qi Li,[‡] Shengli Zhuang,[§] Yongbo Song,[‡] David J. Morris,[⊥] Meng Zhou,[‡] Zhikun Wu,[§] Peng Zhang,[⊥] and Rongchao Jin*[,‡]

[†]Henan Collaborative Innovation Center of Environmental Pollution Control and Ecological Restoration, Zhengzhou University of Light Industry, Zhengzhou 450001, China

[‡]Department of Chemistry, Carnegie Mellon University, Pittsburgh, Pennsylvania 15213, United States

[§]Key Laboratory of Materials Physics, Institute of Solid State Physics, Chinese Academy of Sciences, Hefei 230031, China

[⊥]Department of Chemistry, Dalhousie University, Halifax, Nova Scotia B3R 4J2, Canada

Supporting Information

ABSTRACT: Chemoselective hydrogenation of nitrobenzaldehyde derivatives is one of the important catalytic processes being studied in hydrogenation catalysis. In this work, we report for the first time the catalytic reaction over atomically precise gold nanocluster catalysts (Au_{25}, Au_{38}, Au_{52}, and Au_{144}) using potassium formate as the hydrogen source. A complete selectivity for hydrogenation of the aldehyde group, instead of the nitro group, is obtained. A distinct dependence on the size of nanocluster catalysts is also observed, in which the $Au_{38}(SCH_2CH_2Ph)_{24}$ gives rise to the highest catalytic activity. The catalyst also shows good versatility and recyclability. Interestingly, the ligand-off nanocluster changes its catalytic selectivity to the nitro hydrogenation, which is in contrast with the ligand-on catalyst. In addition, the selectivity can be restored by treating the ligand-off nanocluster catalyst with thiol. This reversible control of chemoselectivity is remarkable and may stimulate future work on the exploitation of such nanoclusters for hydrogenation catalysis with control over selectivity.

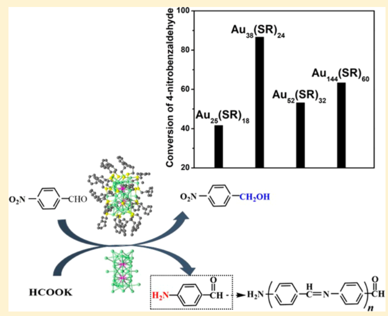

Selective hydrogenation of aldehydes to the corresponding alcohols is an important transformation reaction in both the laboratory and industry.[1−3] There are generally two routes: (i) direct hydrogenation with H_2 under pressure and (ii) transfer hydrogenation using a non-H_2 molecule as the hydrogen source. Because of the elimination of the hazardous, pressured H_2 with the use of easily available hydrogen donors, transfer hydrogenation is an attractive alternative to the direct hydrogenation route and has become a hot area of research in hydrogenation catalysis.[4−6]

It is known that transfer hydrogenation can occur on both homogeneous and heterogeneous catalysts based on iron, cobalt, nickel, rhodium, palladium, gold, etc.[6] From a practical point of view, it is more desirable to develop efficient heterogeneous catalysts for the transformation reaction.[6,7] Compared to other metal catalysts, gold nanocatalysts have attracted increasing attention in the last decades owing to their good activity and extraordinary selectivity in many processes.[8−18] For instance, Cao et al. found that Au nanoparticles supported on CeO_2 and TiO_2 showed high activity and selectivity for the transfer hydrogenation of carbonyl compounds.[15,16] Guo et al. reported that the Au/SiC photocatalyst was capable of catalyzing the hydrogenation of α,β-unsaturated aldehydes to the corresponding unsaturated alcohols with high activity and selectivity using 2-propanol as the hydrogen source.[17] Nanoporous gold was also found to be an efficient catalyst for the chemoselective reduction of α,β-unsaturated aldehydes to the corresponding allylic alcohols with silane.[18] These gold nanoparticles or nanoporous gold catalysts are, however, more or less polydispersed in size, and their structures are not well-defined at the atomic level, which results in difficulties in investigating the precise size-dependent catalytic property and elucidating the structure−property relationships. Therefore, it is highly desirable to design gold nanocatalysts with precise particle sizes and, more importantly, with well-defined atomic structures.

In recent years, well-defined gold nanoclusters protected by thiolate ligands (with core size ranging from 1 to 3 nm) have emerged as a new class of nanomaterials.[19−23] These nanoclusters are of atomic precision and molecular purity, and some of them have been applied in catalytic reactions such as selective oxidation, selective hydrogenation, carbon−carbon coupling, and photocatalytic reactions.[21,23−33] For instance, Zhu et al. obtained ∼100% selectivity for unsaturated alcohols in the hydrogenation of a range of α,β-unsaturated ketones

Received: September 10, 2018
Accepted: December 11, 2018
Published: December 12, 2018

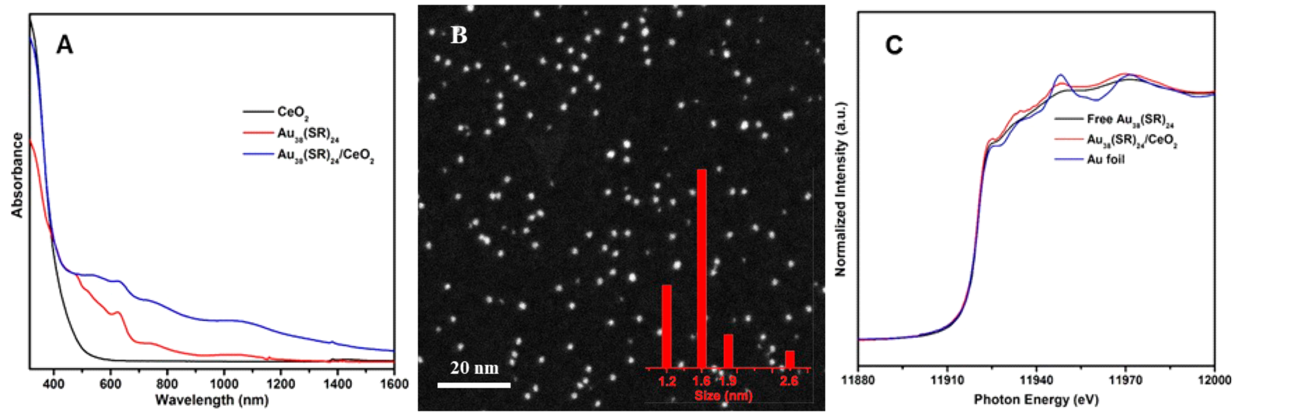

Figure 1. (A) Diffuse reflectance optical spectra of CeO_2 and $Au_{38}(SR)_{24}/CeO_2$, together with the transmission optical spectrum of $Au_{38}(SR)_{24}$ nanoclusters in dichloromethane; (B) HAADF-STEM image of the free $Au_{38}(SR)_{24}$ nanoclusters (inset: size histogram); (C) normalized Au L3-edge XANES spectra of free $Au_{38}(SR)_{24}$ and $Au_{38}(SR)_{24}/CeO_2$.

(except crotonaldehyde) using Au_{25} nanoclusters as the catalysts.[24] For the selective reduction of nitrobenzaldehyde with molecular hydrogen, aminobenzaldehyde was obtained as the main product using the supported gold nanoparticles as catalysts;[34,35] in contrast, nitrobenzyl alcohol was obtained as the sole product using ligand-protected gold nanocluster catalysts.[36−38] These results indicate that gold nanoclusters are promising in the development of novel hydrogenation catalysts[27−29,36−38] or serving as precatalysts.[39−41] For the latter, Zhang et al. recently reported ZnAl-hydrotalcite-supported $Au_{25}(Cys)_{18}$ (Cys = cysteine) as a precatalyst for selective hydrogenation of 3-nitrostyrene over broad windows of reaction duration and temperature, in which excellent selectivity (>98%) to 3-vinylaniline at complete conversion was attained.[41]

Research progress in atomically precise nanoclusters has led to a series of nanoclusters with their total structures determined by X-ray crystallography.[21] The atomic-level structures (metal core plus surface ligands) offer unprecedented opportunities for deep understanding of the size- and structure-dependent activity of gold nanocluster catalysts and also precise correlation of the catalytic properties with the structures.[33] Recently, Bhattacharjee et al. performed density functional theory calculations on the catalytic transfer reduction of aldehydes to alcohols catalyzed by bare gold nanoclusters supported on TiO_2.[42] However, there is no experimental report yet on transfer hydrogenation catalyzed by atomically precise gold nanoclusters.

Herein, we explore for the first time gold nanoclusters as the transfer hydrogenation catalysts for selective hydrogenation of nitrobenzaldehyde derivatives using potassium formate as the hydrogen source. The nanoclusters studied in this work include $Au_{25}(SR)_{18}$, $Au_{38}(SR)_{24}$, $Au_{52}(SR)_{32}$, and $Au_{144}(SR)_{60}$ (where R = CH_2CH_2Ph). A complete selectivity (∼100%) for the aldehyde group is achieved. Among the investigated gold nanoclusters, a distinct size dependence of the catalytic activity is found, with $Au_{38}(SR)_{24}$ exhibiting the highest catalytic activity. Furthermore, a reversible control of the chemoselectivity is achieved, with the ligand-on nanoclusters for selective −CHO hydrogenation and the ligand-off nanoclusters for selective $-NO_2$ hydrogenation. This reversible control of selectivity provides a unique strategy for hydrogenation catalysis.

The syntheses of $Au_{25}(SR)_{18}$, $Au_{38}(SR)_{24}$, $Au_{52}(SR)_{32}$, and $Au_{144}(SR)_{60}$ nanoclusters follow the literature methods.[20,43−45] All of these nanoclusters are protected by the same ligand (i.e., R = CH_2CH_2Ph), and their atomic structures (except $Au_{144}(SR)_{60}$) have been determined by X-ray crystallography[44,46,47] as well as X-ray spectroscopic analyses.[48−50] The oxide-supported $Au_n(SR)_m$ nanocluster catalysts (1 wt % loading of ligand-protected clusters) are obtained by impregnation of oxide powders in CH_2Cl_2 solutions of nanoclusters and then annealed at 150 °C for 1.0 h under vacuum.

Here the $Au_{38}(SR)_{24}/CeO_2$ catalyst is chosen as an example for detailed discussions of characterization. The electrospray mass spectrum of solution-phase $Au_{38}(SR)_{24}$ shows its atomic precision (Figure S1). The diffuse UV−vis−NIR spectrum of $Au_{38}(SR)_{24}/CeO_2$ exhibits a series of peaks at 1050, 750, 620, and 520 nm (Figure 1A, blue profile), which match well with the spectroscopic "fingerprints" of pure $Au_{38}(SR)_{24}$ in solution (Figure 1A, red profile),[43] indicating that the deposited $Au_{38}(SR)_{24}$ nanoclusters on CeO_2 remain intact (i.e., no aggregation or metal core structural change); however, the surface ligands can fan out, resulting in adsorption interactions between the cluster and the support. The shorter-wavelength portion (<500 nm) in the spectrum is dominated by the band gap absorption of CeO_2 (c.f. the black profile of plain CeO_2 in Figure 1A). Thermogravimetric analysis (TGA) of unsupported $Au_{38}(SR)_{24}$ shows that the thiolate ligands start to desorb at ∼200 °C;[51] other sizes show a similar desorption temperature.[45] These results imply that the 150 °C annealing process (the pretreatment step) should not lead to desorption of thiolate ligands because the temperature is 50 °C below the desorption temperature. High-angle annular dark-field scanning transmission electron microscopy (HAADF-STEM) imaging shows that the size of free $Au_{38}(SR)_{24}$ nanoclusters is comparable to the size measured by X-ray crystallography (Figure 1B).[47] It is worth noting that a small fraction of larger sized particles are observed, which are caused by high-energy e-beam irradiation (i.e., agglomeration of $Au_{38}(SR)_{24}$ nanoclusters). For the supported $Au_{38}(SR)_{24}/CeO_2$, gold nanoclusters were hard to observe because of the insufficient Z-contrast between ultrasmall Au_{38} and large sized CeO_2 particles (Figure S2a,b), but the elemental maps show Au, Ce, and O (Figure S2c). Here, we employed X-ray absorption spectroscopy[48−50] to analyze the local geometric and electronic

DOI: 10.1021/acs.jpclett.8b02784
J. Phys. Chem. Lett. 2018, 9, 7173−7179

Table 1. Transfer Hydrogenation of 4-Nitrobenzaldehyde over $Au_{38}(SR)_{24}$/Oxide ($R = CH_2CH_2Ph$)[a]

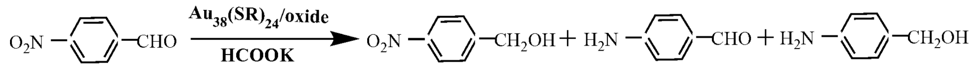

1 2 3

entry	catalyst	conv. (%)[e]	sel. (%)[e]		
			1	2	3
1	$Au_{38}(SR)_{24}/SiO_2$	1.5	~100	n.d.	n.d.
2	$Au_{38}(SR)_{24}/TiO_2$	16.0	~100	n.d.	n.d.
3	$Au_{38}(SR)_{24}/CeO_2$	86.7	~100	n.d.	n.d.
4	CeO_2	2.3	~100	n.d.	n.d.
5[b]	$Au_{38}(SR)_{24}/CeO_2$	91.0	~100	n.d.	n.d.
6[c]	$Au_{38}(SR)_{24}/CeO_2$	90.2	~100	n.d.	n.d.
7[d]	$Au_{38}(SR)_{24}/CeO_2$	90.0	~100	n.d.	n.d.

[a]Conditions: 100 mg of $Au_{38}(SR)_{24}$/oxide (1 wt % loading), 1 mL of H_2O, 0.05 mmol 4-nitrobenzaldehyde, 0.25 mmol HCOOK, 80 °C, 12 h. [b]90 °C. [c]The results of the second use. [d]The results of the third use. [e]The conversion of 4-nitrobenzaldehyde and the selectivity for 4-nitrobenzyl alcohol were determined by ^{1}H NMR analysis. No other product was detected (abbreviated as n.d.), and about 95% mass balance of 4-nitrobenzyl alcohol was obtained by using an o-xylene internal standard.

structures of the supported nanoclusters after the $Au_{38}(SR)_{24}/CeO_2$ catalyst was annealed at 150 °C for 1 h in vacuum. As shown in Figure 1C, the X-ray absorption near-edge structure (XANES) spectra of the free $Au_{38}(SR)_{24}$ nanoclusters and the annealed $Au_{38}(SR)_{24}/CeO_2$ catalyst are essentially identical in the profile (Figure 1C, black and red curves), indicating that the geometric and electronic structures of supported $Au_{38}(SR)_{24}$ nanoclusters are unaltered after the 150 °C pretreatment. The slight difference in the XANES features of the free (i.e., unsupported) and supported nanoclusters is caused by the nanocluster−CeO_2 interactions.[52,53] The EXAFS spectra of unsupported $Au_{38}(SR)_{24}$ and $Au_{38}(SR)_{24}/CeO_2$ also showed no apparent increase of cluster size after the 150 °C annealing (Supporting Information, Figure S3). In previous research, IR and X-ray absorption spectroscopy characterizations reported that $Au_n(SR)_m$ nanoclusters on CeO_2 rods remained intact after thermal treatment at 150 °C in air.[26] All the results confirm that the $Au_{38}(SR)_{24}$ nanoclusters supported on CeO_2 did not decompose or grow to larger particles during the thermal treatment (150 °C).

To evaluate the catalytic properties of gold nanoclusters, we chose the selective hydrogenation of 4-nitrobenzaldehyde by potassium formate (HCOOK) as a model reaction (Table 1). The transfer hydrogenation process employs the readily available potassium formate as the hydrogen source, instead of the highly flammable and explosive molecular hydrogen, and furthermore it is carried out in water at relatively mild conditions. Such a process is advantageous and eco-friendly compared with the reported catalytic hydrogenation process in organic solvents.[33−35] It is worth noting that CO_2 is generated after the hydrogen transfer from HCOOK.

All the supported gold nanoclusters showed ~100% selectivity for the 4-nitrobenzyl alcohol product (Table 1). It is worth comparing with previous reports on conventional nanogold catalysts for the transfer hydrogenation reactions,[54−56] in which reactants containing a nitro group and another reducible group (e.g., aldehyde group) exclusively gave rise to products with the reduction of the nitro group. Therefore, the reduction of the aldehyde group in our system, instead of the nitro group, is surprising and indicates the unexpected properties of $Au_n(SR)_m$ nanoclusters.

The CeO_2 support exhibits a negligible activity (Table 1, entry 4). Among the SiO_2, TiO_2, and CeO_2 supports, CeO_2 is found to be the best one, while SiO_2 or TiO_2 supported nanoclusters gave very low activity (1.5% and 16.0%, respectively). The highest activity with 86.7% conversion was achieved over the $Au_{38}(SR)_{24}/CeO_2$ catalyst. When raising the temperature to 90 °C, the activity can be further improved to 91.0% (Table 1, entry 5). It is known that SiO_2 is acidic and TiO_2 is amphoteric, while CeO_2 is basic. Therefore, the high catalytic activity of $Au_{38}(SR)_{24}/CeO_2$ should be related to the base properties of CeO_2. Given the fact that plain CeO_2 (i.e., without nanoclusters) offers only a ~2% conversion, the high activity of $Au_{38}(SR)_{24}/CeO_2$ indicates a distinct synergy between the nanocluster and CeO_2, in particular, the role of CeO_2 in mediating the activation of the hydrogen source (see mechanistic discussions below).

For a comparison with the ligand-on gold nanoclusters that exhibit a complete selectivity (~100%) for the aldehyde group, we further prepared and characterized the ligand-off, CeO_2-supported Au_{38} nanoclusters by thermal treatment (300 °C, 1.5 h) of $Au_{38}(SR)_{24}/CeO_2$ and then employed the ligand-off catalyst in the transfer hydrogenation of 4-nitrobenzaldehyde under otherwise identical reaction conditions. After the thermal treatment at 300 °C, the white line region of X-ray absorption between 11920 and 11925 eV dropped in intensity as a result of the ligand removal (Figure S4) and becomes closer to the feature of Au foil, which indicates that the majority of Au sites of $Au_{38}(SR)_{24}/CeO_2$ is in the metallic state. According the EXAFS spectra of ligand-off Au_{38} and reference samples (Figure S5), the ligand-off nanoclusters have grown to larger particles after the 300 °C treatment. HAADF-STEM images also show a size range from 2.0 to 5.2 nm, in accordance with the above result (Figure S6). For the catalytic reaction, we found that 4-nitrobenzaldehyde was exhausted, but none of the three products was detected by ^{1}H NMR; instead we observed the appearance of an insoluble product. This phenomenon is ascribed to the polymerization of 4-aminobenzaldehyde to yield polymeric products as previously reported.[34,57,58] We rationalize that when using ligand-off gold nanoclusters as the catalyst, 4-aminobenzaldehyde is first generated because of the reduction of the nitro group, and this product is soon consumed by a polymerization process.

Because of its easy polymerization, 4-aminobenzaldehyde is not available commercially, and thus, one cannot directly test it as a substrate to prove the polymerization process. To confirm

DOI: 10.1021/acs.jpclett.8b02784
J. Phys. Chem. Lett. 2018, 9, 7173−7179

Scheme 1. Proposed Pathway for the Polymer Formation in Transfer Hydrogenation of 4-Nitrobenzaldehyde Catalyzed by Ligand-off Gold Nanoclusters

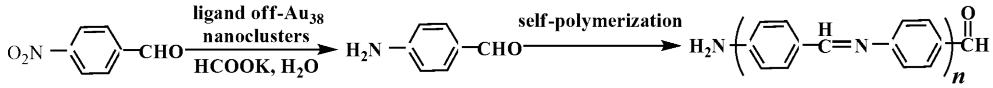

the possibility of the polymer formation, herein the hydrogenation of 4-nitrobenzaldehyde over the Au/NiAl-oxide catalyst as a control experiment was carried out under the pressure of 10 atm H_2 for 4 h. The chemical composition of the reaction solution was analyzed by ESI-MS and GC (Figure S7). Because of the difficulty in attaching or losing a hydrogen ion, it is hard for a molecule containing a NO_2 group to form the charged ion. Therefore, the mass peak for 4-nitrobenzaldehyde (M = 151.12) was not observed, although there is still a certain amount of 4-nitrobenzaldehyde detected by GC. Two mass peaks were found at 122.14 and 225.10; the former is assigned to 4-aminobenzaldehyde (M = 121.14), and the latter is assigned to the dimer (M = 224.26), which originate from the self-polymerization of 4-amino benzaldehyde, in accordance with the published research.[34,58] In addition, a certain amount of insoluble product appeared in the reaction solution after the solution was allowed to stand for ∼8 h at room temperature. After the insoluble polymer was separated by centrifugation, the reaction solution was determined by ESI-MS (Figure S8). The emergence of the insoluble polymer and the large increase in the relative abundance of the mass peak for the dimeric polymer indicate that 4-aminobenzaldehyde can be consumed to form its dimer even at room temperature. The results show that self-polymerization of the as-obtained 4-aminobenzaldehyde to generate its polymer can take place during the selective hydrogenation of 4-nitrobenzaldehyde. Furthermore, the amount of the polymer increases with the extension of time even at room temperature. Together with the previous reports,[34,57,58] the formation process of the polymer in transfer hydrogenation of 4-nitrobenzaldehyde catalyzed by ligand-off gold nanoclusters is proposed as below (Scheme 1). This should be a reasonable pathway for the polymer formation.

The ligand-off, supported Au_{38} nanoclusters were further treated with phenylethanethiol and then reapplied as the catalyst in the transfer hydrogenation of 4-nitrobenzaldehyde. Interestingly, the as-treated catalyst (i.e., thiol restored) exhibits the same catalytic property (87% conversion of 4-nitrobenzaldehyde with complete selectivity to the aldehyde group) just as the original $Au_{38}(SR)_{24}/CeO_2$ catalyst under the same reaction conditions. This reversibility is quite remarkable. The results confirm that the ligand-on gold nanocluster is responsible for its unique selectivity (∼100%) toward the reduction of the aldehyde group, while the ligand-off catalyst gives rise to the exclusive reduction of the nitro group. The major effects of the presence/absence of ligands on the chemoselective hydrogenation have not been observed in previous work, although in other systems thiolate ligands were found to tune the selectivity of metal catalysts for certain chemical reactions because of active-site selection, molecular recognition, and steric effect,[59,60] and Tsukuda et al. also reported that the presence of thiolates on Au_{25} nanoclusters improved the selectivity for benzaldehyde in the liquid oxidation of benzyl alcohol.[61] In our system, we rationalize that there should be different adsorption modes of 4-nitrobenzaldehyde on the surfaces of ligand-on and ligand-off nanoclusters. Previous theoretical simulations reported that the carbonyl group was adsorbed onto the surface gold atoms of $Au_{25}(SR)_{18}$ in catalytic reduction of CO_2.[62] The unexpected selectivity of the ligand-on nanocluster catalysts should arise from the preferred absorption of the aldehyde group of 4-nitrobenzaldehyde on the exposed gold atoms of $Au_{38}(SR)_{24}$.

We further investigated Au_{25}, Au_{38}, Au_{52}, and Au_{144} nanoclusters. All the sizes exhibited a complete selectivity to the aldehyde group, and a distinct dependence of the catalytic activity on the nanocluster size was also observed (Table 2).

Table 2. Size Dependence of Gold Nanoclusters in Transfer Hydrogenation of 4-Nitrobenzaldehyde[a]

			sel. (%)[b]		
entry	catalyst	conv. (%)[b]	1	2	3
1	$Au_{25}(SR)_{18}/CeO_2$	41.7	∼100	n.d.[c]	n.d.
2	$Au_{38}(SR)_{24}/CeO_2$	86.7	∼100	n.d.	n.d.
3	$Au_{52}(SR)_{32}/CeO_2$	53.2	∼100	n.d.	n.d.
4	$Au_{144}(SR)_{60}/CeO_2$	63.4	∼100	n.d.	n.d.

[a]Conditions: 100 mg of $Au_n(SR)_m/CeO_2$ (1 wt % loading), 1 mL of H_2O, 0.05 mmol 4-nitrobenzaldehyde, 0.25 mmol HCOOK, 80 °C, 12 h. [b]The conv. of 4-nitrobenzaldehyde and sel. for 4-nitrobenzyl alcohol were determined by ^1H NMR. [c]n.d. = not detected.

Among them, $Au_{38}(SR)_{24}/CeO_2$ displays the highest activity. With the available atomic structures of $Au_{25}(SR)_{18}$, $Au_{38}(SR)_{24}$, and $Au_{52}(SR)_{32}$ (Figure 2), we compared the activity based on the turnover frequencies, which are 0.57, 1.08, and 0.71 h^{-1}, respectively (Table S1), in which $Au_{38}(SR)_{24}/CeO_2$ still possesses the best catalytic performance. The observed size-dependent activity is not due to the geometrical surface area effect; rather, it is caused by the electronic effect. In contrast, previous work of selective hydrogenation of 4-nitrobenzaldehyde with H_2 as the hydrogen source showed no size dependence using $Au_{25}(SPh)_{18}/CeO_2$, $Au_{36}(SPh)_{24}/CeO_2$, and $Au_{99}(SPh)_{42}/CeO_2$ nanocluster catalysts.[37] Therefore, the observed size dependence implies different catalytic mechanisms for the chemoselective reduction of 4-nitrobenzaldehyde due to different hydrogen sources,

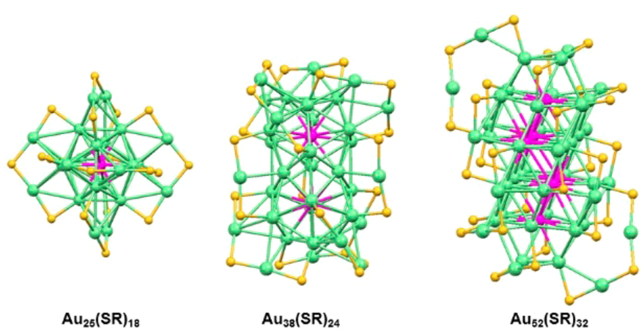

Figure 2. X-ray crystal structures of $Au_{25}(SR)_{18}$, $Au_{38}(SR)_{24}$, and $Au_{52}(SR)_{32}$. Magenta, core Au atoms; light green, exposed surface Au atom; yellow, sulfur (C and H atoms are omitted for clarity).

DOI: 10.1021/acs.jpclett.8b02784
J. Phys. Chem. Lett. 2018, 9, 7173−7179

i.e., H_2 (previous work) versus potassium formate (the present work). The formation of a gold−hydrogen intermediate from H_2 versus HCOOK may exhibit different charge states and hence different hydrogenation modes.

The reusability of the $Au_{38}(SR)_{24}/CeO_2$ catalyst was further studied. After the reaction, the $Au_{38}(SR)_{24}/CeO_2$ catalyst was collected by centrifugation, washed with water and ethyl acetate, and dried in vacuum. Then, the recycled catalyst was recharged with fresh reactants and reused in the reaction. No appreciable loss of activity and selectivity was found in three consecutive uses (no further reuse was tested) (Table 1, entries 6 and 7). Subsequently, the used $Au_{38}(SR)_{24}/CeO_2$ was measured using STEM and X-ray absorption spectroscopy. HAADF-STEM images showed gold nanoclusters were hard to see because of insufficient contrast; the elemental maps showed the Au, Ce, and O (Figure S9). It can be seen that the fresh and used $Au_{38}(SR)_{24}/CeO_2$ showed identical XANES features, suggesting the unchanged structure of $Au_{38}(SR)_{24}/CeO_2$ before and after the hydrogenation reaction (Figure S10). The results demonstrated that the $Au_{38}(SR)_{24}/CeO_2$ catalyst was stable and possessed good recyclability for this transformation reaction.

The scope of substrates was tested to examine the versatility of the $Au_{38}(SR)_{24}/CeO_2$ catalyst (Table 3). First, we

Table 3. Transfer Hydrogenation of Nitrobenzaldehyde Derivatives over $Au_{38}(SR)_{24}/CeO_2$ (R = CH_2CH_2Ph)[a]

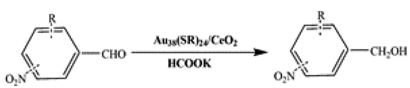

entry	substrate	conv. (%)[b]	sel. (%)[b]
1	4-nitrobenzaldehyde	91.0	100
2	2-nitrobenzaldehyde	30.0	100
3	3-nitrobenzaldehyde	83.6	100
4	4-methyl-3-nitrobenzaldehyde	88.6	100
5	4-chloro-3-nitrobenzaldehyde	86.5	100

[a]Conditions: 100 mg of $Au_n(SR)_m$/oxide (1 wt % loading), 1 mL of H_2O, 0.05 mmol 4-nitrobenzaldehyde, 0.25 mmol HCOOK, 90 °C, 12 h. [b]The conv. of 4-nitrobenzaldehyde and the sel. for 4-nitrobenzyl alcohol were determined by ^{1}H NMR.

investigated the effect of nitro group at the ortho, meta, and para positions and found that *p*-nitrobenzaldehyde gave the highest result among the three nitrobenzaldehyde isomers, while *o*-nitrobenzaldehyde had the lowest conversion (Table 3, entries 1−3). In contrast to the distinct steric effect, we found that the inclusion of electron-rich or deficient group had no significant effect on the conversion of reactants (Table 3, entries 4 and 5). It is noted that the selectivity for the aldehyde group remains ∼100% in all the investigated hydrogenation reactions. Overall, the results show that the catalytic properties of $Au_{38}(SR)_{24}/CeO_2$ are greatly affected by the substituent position of the nitro group (steric effect) but not by the electron-rich or deficient side group.

Scheme 2 shows a proposed mechanism for the potassium formate-mediated transfer hydrogenation of 4-nitrobenzaldehyde over $Au_{38}(SR)_{24}/CeO_2$. The atomic structure of $Au_{38}(SR)_{24}$ comprises a face-fused biicosahedral inner core of Au_{23},[47] which is protected by six dimeric $Au_2(SR)_3$ and three monomeric $Au(SR)_2$ staple-like surface motifs, shown in Figure 2. As mentioned above, the aldehyde group of 4-nitrobenzaldehyde is first adsorbed onto the exposed gold

Scheme 2. Proposed Mechanism for the Potassium Formate-Mediated Transfer Hydrogenation of 4-Nitrobenzaldehyde over the $Au_{38}(SR)_{24}/CeO_2$ Catalyst[a]

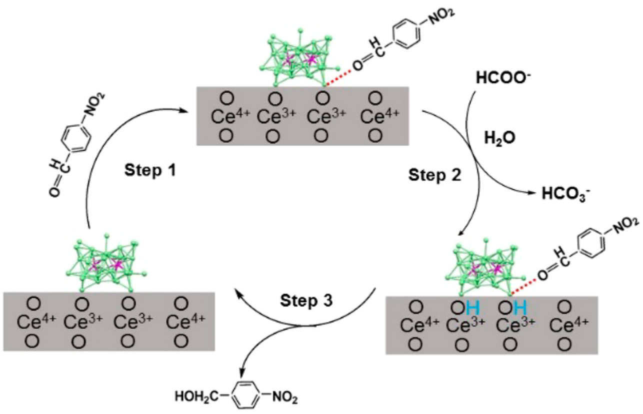

[a]Magenta, core Au atoms; light green, exposed Au atom. (The ligands are omitted for clarity.)

atoms of $Au_{38}(SR)_{24}$, in accordance with previously reported results.[36,37,62] Then, the ceria sites facilitated by H_2O (solvent) are involved in the dehydrogenation of formate to bicarbonate species,[15] and the formed hydrogen species could transfer to the vicinal and exposed gold atoms of the surface shell of gold nanoclusters by a process of reverse hydrogen spillover.[63,64] Indeed, recent work by Tsukuda et al. has observed the Au−H in ligand-protected gold nanoclusters.[65] The hydride further interacts with the adsorbed 4-nitrobenzaldehyde, thereby giving rise to the 4-nitrobenzyl alcohol product.[66] Overall, the interface between the nanocluster and CeO_2 should play an important role in dehydrogenating formate to form the hydride species and transferring the hydride to the gold nanocluster for subsequent hydrogenation of the HC=O group selectively. Note that our proposed mechanism is worthy of being thoroughly investigated in future work.

In summary, chemoselective transfer hydrogenation of nitrobenzaldehyde derivatives is achieved for the first time with atomically precise gold nanocluster catalysts using potassium format as the hydrogen source. A complete selectivity for the aldehyde group and excellent activity are obtained for a range of substrates (except *o*-nitrobenzaldehyde). Among the nanocluster catalysts, $Au_{38}(SR)_{24}/CeO_2$ gives the highest catalytic activity, indicating a distinct size dependence. The catalyst shows good versatility for substrates and also good recyclability. The catalytic properties of $Au_{38}(SR)_{24}/CeO_2$ should originate from the cluster-activated nitrobenzaldehyde derivatives and CeO_2-activated HCOOK. Compared with the H_2 route, the transfer hydrogenation process over $Au_{38}(SR)_{24}/CeO_2$ is advantageous as it is carried out in water at relatively mild conditions with the easily available potassium formate as the hydrogen source. An atomic-level understanding of the structure−property relationship will enable the rational design of efficient gold nanostructured catalysts.

■ ASSOCIATED CONTENT

Supporting Information

The Supporting Information is available free of charge on the ACS Publications website at DOI: 10.1021/acs.jpclett.8b02784.

DOI: 10.1021/acs.jpclett.8b02784
J. Phys. Chem. Lett. 2018, 9, 7173−7179

Experimental details and characterizations of some catalysts (PDF)

■ AUTHOR INFORMATION

Corresponding Author

*E-mail: rongchao@andrew.cmu.edu.

ORCID

Meng Zhou: 0000-0001-5187-9084

Zhikun Wu: 0000-0002-2711-3860

Peng Zhang: 0000-0003-3603-0175

Rongchao Jin: 0000-0002-2525-8345

Notes

The authors declare no competing financial interest.

■ ACKNOWLEDGMENTS

J.Z. acknowledges financial support from the National Natural Science Foundation of China (21576248), a research fund from the doctoral program of Zhengzhou University of Light Industry (2014BSJJ007), and Scientific and Technological Project of Henan Province (152102210355). Z.W. acknowledges the Natural Science Foundation of China (No. 21528303). R.J. acknowledges financial support from the U.S. National Science Foundation (DMREF-0903225). This research used resources of the Advanced Photon Source, an Office of Science User Facility operated for the U.S. DOE Office of Science by Argonne National Laboratory, and was supported by the U.S. DOE under Contract No. DE-AC02-06CH11357 and the Canadian Light Source and its funding partners. XAS technical support from Dr. Zou Finfrock is also acknowledged.

■ REFERENCES

(1) Bailie, J. E.; Hutchings, G. J. Promotion by sulfur of gold catalysts for crotyl alcohol formation from crotonaldehyde hydrogenation. *Chem. Commun.* **1999**, 2151−2152.

(2) Ikariya, T.; Blacker, A. J. Asymmetric transfer hydrogenation of ketones with bifunctional transition metal-based molecular catalysts. *Acc. Chem. Res.* **2007**, *40*, 1300−1308.

(3) Mitsudome, T.; Kaneda, K. Gold nanoparticle catalysts for selective hydrogenations. *Green Chem.* **2013**, *15*, 2636−2654.

(4) Brieger, G.; Nestrick, T. J. Catalytic transfer hydrogenation. *Chem. Rev.* **1974**, *74*, 567−580.

(5) Gladiali, S.; Al-berico, E. Asymmetric transfer hydrogenation: chiral ligands and applications. *Chem. Soc. Rev.* **2006**, *35*, 226−236.

(6) Wang, D.; Astruc, D. The golden age of transfer hydrogenation. *Chem. Rev.* **2015**, *115*, 6621−6686.

(7) Selvam, P.; Sonavane, S. U.; Mohapatra, S. K.; Jayaram, R. V. Chemoselective reduction of α,β-unsaturated carbonyls over novel mesoporous CoHMA molecular sieves under hydrogen transfer conditions. *Adv. Synth. Catal.* **2004**, *346*, 542−544.

(8) Haruta, M.; Kobayashi, T.; Sano, H.; Yamada, N. Novel gold catalysts for the oxidation of carbon monoxide at a temperature far below 0 °C. *Chem. Lett.* **1987**, *16*, 405−408.

(9) Jin, R. The impacts of nanotechnology on catalysis by precious metal nanoparticles. *Nanotechnol. Rev.* **2012**, *1*, 31−56.

(10) Pina, C. D.; Falletta, E.; Rossi, M. Update on selective oxidation using gold. *Chem. Soc. Rev.* **2012**, *41*, 350−369.

(11) Sun, K. Q.; Hong, Y. C.; Zhang, G. R.; Xu, B. Q. Synergy between Pt and Au in Pt-on-Au nanostructures for chemoselective hydrogenation catalysis. *ACS Catal.* **2011**, *1*, 1336−1346.

(12) Ta, N.; Liu, J.; Chenna, S.; Crozier, P. A.; Li, Y.; Chen, A.; Shen, W. Stabilized gold nano-particles on ceria nanorods by strong interfacial anchoring. *J. Am. Chem. Soc.* **2012**, *134*, 20585−20588.

(13) Zhao, J. B.; Yu, G.; Xin, K.; Li, L.; Fu, T.; Cui, Y.; Liu, H.; Xue, N.; Peng, L.; Ding, W. Highly active gold catalysts loaded on NiAl-oxide derived from layered double hydroxide for aerobic alcohol oxidation. *Appl. Catal., A* **2014**, *482*, 294−299.

(14) Khetrapal, N. S.; Wang, L.-S.; Zeng, X. C. Determination of CO adsorption sites on gold clusters Au_n^- (n = 21−25): A size region that bridges the pyramidal and core-shell structures. *J. Phys. Chem. Lett.* **2018**, *9*, 5430−5439.

(15) He, L.; Ni, J.; Wang, L. C.; Yu, F. J.; Cao, Y.; He, H. Y.; Fan, K. N. Aqueous room-temperature gold-catalyzed chemoselective transfer hydrogenation of aldehydes. *Chem. - Eur. J.* **2009**, *15*, 11833−11836.

(16) Su, F. Z.; He, L.; Ni, J.; Cao, Y.; He, H. Y.; Fan, K. N. Efficient and chemoselective reduction of carbonyl compounds with supported gold catalysts under transfer hydrogenation conditions. *Chem. Commun.* **2008**, *44*, 3531−3533.

(17) Hao, C. H.; Guo, X. N.; Pan, Y. T.; Chen, S.; Jiao, Z. F.; Yang, H.; Guo, X. Y. Visible-light-driven selective photocatalytic hydrogenation of cinnamaldehyde over Au/SiC catalysts. *J. Am. Chem. Soc.* **2016**, *138*, 9361−9364.

(18) Takale, B. S.; Wang, S.; Zhang, X.; Feng, X.; Yu, X.; Jin, T.; Bao, M.; Yamamoto, Y. Chemoselective reduction of α, β-unsaturated aldehydes using an unsupported nanoporous gold catalyst. *Chem. Commun.* **2014**, *50*, 14401−14404.

(19) Negishi, Y.; Nobusada, K.; Tsukuda, T. Glutathione-protected gold clusters revisited: bridging the gap between gold(I)-thiolate complexes and thiolate-protected gold nano-crystals. *J. Am. Chem. Soc.* **2005**, *127*, 5261−5270.

(20) Zhu, M.; Lanni, E.; Garg, N.; Bier, M. E.; Jin, R. Kinetically controlled, high-yield synthesis of Au_{25} clusters. *J. Am. Chem. Soc.* **2008**, *130*, 1138−1139.

(21) Jin, R.; Zeng, C.; Zhou, M.; Chen, Y. Atomically precise colloidal metal nanoclusters and nanoparticles: fundamentals and opportunities. *Chem. Rev.* **2016**, *116*, 10346−10413.

(22) Zeng, C.; Chen, Y.; Kirschbaum, K.; Lambright, K. J.; Jin, R. Emergence of hierarchical structural complexities in nanoparticles and their assembly. *Science* **2016**, *354*, 1580−1584.

(23) Li, W.; Ge, Q.; Ma, X.; Chen, Y.; Zhu, M.; Xu, H.; Jin, R. Mild activation of CeO_2-supported gold nanoclusters and insight into the catalytic behavior in CO oxidation. *Nanoscale* **2016**, *8*, 2378−2385.

(24) Zhu, Y.; Qian, H.; Drake, B. A.; Jin, R. Atomically precise $Au_{25}(SR)_{18}$ nanoparticles as catalysts for the selective hydrogenation of alpha, beta-unsaturated ketones and aldehydes. *Angew. Chem., Int. Ed.* **2010**, *49*, 1295−1298.

(25) Liu, Y.; Tsunoyama, H.; Akita, T.; Xie, S.; Tsukuda, T. Aerobic oxidation of cyclohexane catalyzed by size-controlled Au clusters on hydroxyapatite: size effect in the sub-2 nm regime. *ACS Catal.* **2011**, *1*, 2−6.

(26) Wu, Z. L.; Jiang, D. E.; Mann, A. K. P.; Mullins, D. R.; Qiao, Z. A.; Allard, L. F.; Zeng, C. J.; Jin, R.; Overbury, S. H. Thiolate ligands as a double-edged sword for CO oxidation on CeO_2 supported $Au_{25}(SCH_2CH_2Ph)_{18}$ nanoclusters. *J. Am. Chem. Soc.* **2014**, *136*, 6111−6122.

(27) Li, J.; Nasaruddin, R. R.; Feng, Y.; Yang, J.; Yan, N.; Xie, J. Tuning the accessibility and activity of $Au_{25}(SR)_{18}$ nanocluster catalysts through ligand engineering. *Chem. - Eur. J.* **2016**, *22*, 14816−14820.

(28) Shivhare, A.; Ambrose, S. J.; Zhang, H.; Purves, R. W.; Scott, R. W. J. Stable and recyclable Au_{25} clusters for the reduction of 4-nitrophenol. *Chem. Commun.* **2013**, *49*, 276−278.

(29) Li, G.; Jin, R. Gold nanocluster-catalyzed semihydrogenation: a unique activation pathway for terminal alkynes. *J. Am. Chem. Soc.* **2014**, *136*, 11347−11354.

(30) Abroshan, H.; Li, G.; Lin, J.; Kim, H. J.; Jin, R. Molecular mechanism for the activation of $Au_{25}(SCH_2CH_2Ph)_{18}$ nanoclusters by imidazolium-based ionic liquids for catalysis. *J. Catal.* **2016**, *337*, 72−79.

(31) Sakai, N.; Tatsuma, T. Photovoltaic properties of glutathione-protected gold clusters adsorbed on TiO_2 electrodes. *Adv. Mater.* **2010**, *22*, 3185−3188.

DOI: 10.1021/acs.jpclett.8b02784
J. Phys. Chem. Lett. 2018, 9, 7173−7179

(32) Chen, H.; Liu, C.; Wang, M.; Zhang, C.; Luo, N.; Wang, Y.; Abroshan, H.; Li, G.; Wang, F. Visible light gold nanocluster photocatalyst: selective aerobic oxidation of amines to imines. *ACS Catal.* **2017**, *7*, 3632−3638.
(33) Zhao, J.; Jin, R. Heterogeneous catalysis by gold and gold-based bimetal nanoclusters. *Nano Today* **2018**, *18*, 86−102.
(34) Corma, A.; Serna, P. Chemoselective hydrogenation of nitro compounds with supported gold catalysts. *Science* **2006**, *313*, 332−334.
(35) Liu, L.; Qiao, B.; Ma, Y.; Zhang, J.; Deng, Y. Ferric hydroxide supported gold subnano clusters or quantum dots: enhanced catalytic performance in chemoselective hydrogenation. *Dalton Trans* **2008**, 2542−2548.
(36) Li, G.; Jiang, D.; Kumar, S.; Chen, Y.; Jin, R. Size dependence of atomically precise gold nanoclusters in chemoselective hydrogenation and active site structure. *ACS Catal.* **2014**, *4*, 2463−2469.
(37) Li, G.; Zeng, C.; Jin, R. Thermally robust $Au_{99}(SPh)_{42}$ nanoclusters for chemoselective hydrogenation of nitrobenzaldehyde derivatives in water. *J. Am. Chem. Soc.* **2014**, *136*, 3673−3679.
(38) Cano, I.; Chapman, A. M.; Ura-kawa, A.; van Leeuwen, P. W. N. M. Air-stable gold nanoparticles ligated by secondary phosphine oxides for the chemoselective hydrogenation of aldehydes: crucial role of the ligand. *J. Am. Chem. Soc.* **2014**, *136*, 2520−2528.
(39) Ma, G.; Binder, A.; Chi, M.; Liu, C.; Jin, R.; Jiang, D.; Fan, J.; Dai, S. Stabilizing gold clusters by heterostructured transition-metal oxide-mesoporous silica supports for enhanced catalytic activities for CO oxidation. *Chem. Commun.* **2012**, *48*, 11413−11415.
(40) Wang, S.; Yin, S.; Chen, G.; Li, L.; Zhang, H. Nearly atomic precise gold nanoclusters on nickel-based layered double hydroxides for extraordinarily efficient aerobic oxidation of alcohols. *Catal. Sci. Technol.* **2016**, *6*, 4090−4104.
(41) Tan, Y.; Liu, X. Y.; Zhang, L.; Wang, A.; Li, L.; Pan, X.; Miao, S.; Haruta, M.; Wei, H.; Wang, H.; et al. ZnAl-Hydrotalcite supported Au_{25} nanoclusters as precatalysts for chemoselective hydrogenation of 3-nitrostyrene. *Angew. Chem., Int. Ed.* **2017**, *56*, 2709−2713.
(42) Bhattacharjee, R.; Datta, A. Supported sub-nanometer gold cluster catalyzed transfer hydrogenation of aldehydes to alcohols. *J. Phys. Chem. C* **2016**, *120*, 24449−24456.
(43) Qian, H.; Zhu, Y.; Jin, R. Size-focusing synthesis, optical and electrochemical properties of monodisperse $Au_{38}(SC_2H_4Ph)_{24}$ nanoclusters. *ACS Nano* **2009**, *3*, 3795−3803.
(44) Zhuang, S.; Liao, L.; Li, M. B.; Yao, C.; Zhao, Y.; Dong, H.; Li, J.; Deng, H.; Li, L.; Wu, Z. The fcc structure isomerization in gold nanoclusters. *Nanoscale* **2017**, *9*, 14809−14813.
(45) Qian, H.; Jin, R. Controlling nanoparticles with atomic precision: the case of $Au_{144}(SCH_2CH_2Ph)_{60}$. *Nano Lett.* **2009**, *9*, 4083−4087.
(46) Zhu, M.; Aikens, C. M.; Hollander, F. J.; Schatz, G. C.; Jin, R. Correlating the crystal structure of a thiol-protected Au_{25} cluster and optical properties. *J. Am. Chem. Soc.* **2008**, *130*, 5883−5885.
(47) Qian, H.; Eckenhoff, W. T.; Zhu, Y.; Pintauer, T.; Jin, R. Total structure determination of thiolate-protected Au_{38} nanoparticles. *J. Am. Chem. Soc.* **2010**, *132*, 8280−8281.
(48) MacDonald, M. A.; Zhang, P.; Qian, H.; Jin, R. Site-specific and size-dependent bonding of compositionally precise gold-thiolate nanoparticles from X-ray spectroscopy. *J. Phys. Chem. Lett.* **2010**, *1*, 1821−1825.
(49) MacDonald, M. A.; Zhang, P.; Chen, N.; Qian, H.; Jin, R. Solution-phase structure and bonding of $Au_{38}(SR)_{24}$ nanoclusters from X-ray absorption spectroscopy. *J. Phys. Chem. C* **2011**, *115*, 65−69.
(50) MacDonald, M. A.; Chevrier, D.; Zhang, P.; Qian, H.; Jin, R. The structure and bonding of $Au_{25}(SR)_{18}$ nanoclusters from EXAFS: the interplay of metallic and molecular behavior. *J. Phys. Chem. C* **2011**, *115*, 15282−15287.
(51) Qian, H.; Zhu, M.; Andersen, U. N.; Jin, R. Facile, Large-scale synthesis of dodecanethiol-stabilized Au_{38} clusters. *J. Phys. Chem. A* **2009**, *113*, 4281−4284.
(52) Fu, Q.; Saltsburg, H.; Flytzani-Stephanopoulos, M. Active nonmetallic Au and Pt species on ceria-based water-gas shift catalysts. *Science* **2003**, *301*, 935−938.
(53) Si, R.; Flytzani-Stephanopoulos, M. Shape and crystal-plane effects of nanoscale ceria on the activity of Au-CeO_2 catalysts for the water-gas shift reaction. *Angew. Chem., Int. Ed.* **2008**, *47*, 2884−2887.
(54) Liu, X.; Ye, S.; Li, H. Q.; Liu, Y. M.; Cao, Y.; Fan, K. N. Mild, selective and switchable transfer reduction of nitroarenes catalyzed by supported gold nanoparticles. *Catal. Sci. Technol.* **2013**, *3*, 3200−3206.
(55) Guo, H.; Yan, X.; Zhi, Y.; Li, Z.; Wu, C.; Zhao, C.; Wang, J.; Yu, Z.; Ding, Y.; He, W.; et al. Nanostructuring gold wires as highly durable nanocatalysts for selective reduction of nitro compounds and azides with organosilanes. *Nano Res.* **2015**, *8*, 1365−1372.
(56) Yu, L.; Zhang, Q.; Li, S. S.; Huang, J.; Liu, Y. M.; He, H. Y.; Cao, Y. Gold-catalyzed reductive transformation of nitro compounds using formic acid: mild, efficient, and versatile. *ChemSusChem* **2015**, *8*, 3029−3035.
(57) Kimura, K.; Zhuang, J. H.; Kida, M.; Yamashita, Y.; Sakaguchi, Y. Self-assembling polycondensation of 4-aminobenzaldehyde. preparation of star-like aggregates of cone-shaped poly(azomethine) crystals. *Polym. J.* **2003**, *35*, 455−459.
(58) Corma, A.; Serna, P. Preparation of substituted anilines from nitro compounds by using supported gold catalysts. *Nat. Protoc.* **2007**, *1*, 2590−2595.
(59) Schoenbaum, C. A.; Schwartz, D. K.; Medlin, J. W. Controlling the surface environment of heterogeneous catalysts using self-assembled monolayers. *Acc. Chem. Res.* **2014**, *47*, 1438−1445.
(60) Huang, W.; Hua, Q.; Cao, T. Influence and removal of capping ligands on catalytic colloidal nanoparticles. *Catal. Lett.* **2014**, *144*, 1355−1369.
(61) Yoskamtorn, T.; Yamazoe, S.; Takahata, R.; Nishigaki, J.-I.; Thivasasith, A.; Limtrakul, J.; Tsukuda, T. Thiolate-mediated selectivity control in aerobic alcohol oxidation by porous carbon-supported Au_{25} clusters. *ACS Catal.* **2014**, *4*, 3696−3700.
(62) Kauffman, D. R.; Alfonso, D.; Matranga, C.; Qian, H.; Jin, R. Experimental and computational investigation of Au_{25} clusters and CO_2: a unique interaction and enhanced electrocatalytic activity. *J. Am. Chem. Soc.* **2012**, *134*, 10237−10243.
(63) Abad, A.; Almela, C.; Corma, A.; Garcia, H. Unique gold chemoselectivity for the aerobic oxidation of allylic alcohols. *Chem. Commun.* **2006**, *30*, 3178−3180.
(64) Conte, M.; Miyamura, H.; Kobayashi, S.; Chechik, V. Spin trapping of Au-H intermediate in the alcohol oxidation by supported and unsupported gold catalysts. *J. Am. Chem. Soc.* **2009**, *131*, 7189−7196.
(65) Takano, S.; Hirai, H.; Muramatsu, S.; Tsukuda, T. Hydride-doped gold superatom $(Au_9H)^{2+}$: synthesis, structure, and transformation. *J. Am. Chem. Soc.* **2018**, *140*, 8380−8383.
(66) Ouyang, R.; Jiang, D. Understanding selective hydrogenation of α, β-unsaturated ketones to unsaturated alcohols on the $Au_{25}(SR)_{18}$ cluster. *ACS Catal.* **2015**, *5*, 6624−6629.

DOI: 10.1021/acs.jpclett.8b02784
J. Phys. Chem. Lett. 2018, 9, 7173−7179